Multi-dimensional Particle filter-based estimation of inter-system phase biases for multi-GNSS real-time integer ambiguity resolution

Yumiao Tian[1, 5] Zhizhao Liu✉[2] Maorong Ge[3] Frank Neitzel[4]

[1]Faculty of Geosciences and Environmental Engineering, Southwest Jiaotong University, Chengdu, Sichuan, 611756, China

[2]Room ZS617, Block Z, Department of Land Surveying & Geo-Informatics (LSGI), The Hong Kong Polytechnic University (PolyU)

11 Yuk Choi Road, Hung Hom, Kowloon, Hong Kong, China

[3]German Research Centre for Geosciences, 14473 Potsdam, Germany

[4]Institute of Geodesy and Geoinformation Science, Technische Universität Berlin, Berlin, 10623, Germany

[5]State-Province Joint Engineering Laboratory of Spatial Information Technology for High-Speed Railway Safety, Chengdu, Sichuan, 611756, China

Abstract In multi-GNSS integration, fixing inter-system double difference (DD) ambiguities to integers is still a challenge due to the existence of inter-system biases (ISB) when mixed types of GNSS receivers are used. It has been shown that when ISB is known, the inter-system ambiguities can be fixed and the reliability of ambiguity fixing can be improved significantly, especially under poor conditions when the number of observed satellites is small. In traditional methods, the intra-system ambiguity is fixed first then the ISB is estimated to ultimately fix the inter-system ambiguity. In our work, we use the particle-filter-based method to estimate the ISB parameter and fix the inter-system ambiguities to integers at the same time. This method shows higher reliability and higher ambiguity fixing rate. Nevertheless, the existing particle-filter approach for ISB parameter estimation is a one-dimensional algorithm. When satellites from three or more systems are observed, there are two or more ISB parameters. We extend the current one-dimensional particle-filter approach to multi-dimensional case and estimate multi-ISB parameters in this study. We first present a multi-dimensional particle-filter approach that can estimate multi-ISB parameters simultaneously. We also show that the RATIO values can be employed to judge the quality of multi-dimensional ISB values. Afterwards, a two-dimensional particle-filter approach is taken as an example to validate this approach. For example, in the experiment of GPS L5, Galileo E5a and QZSS L5 integration with 6 satellites using the IGS baseline SIN0-SIN1, only three ambiguities are resolved to integer when the ISBs are unknown. The integer ambiguity fixing rate is 41.0% with 53% of the ambiguity fixed solutions have

positioning errors larger than 3 cm. However, when our approach is adopted, the number of integer ambiguity parameters increases to five. The integer ambiguity fixing rate increases to 99.7% with 100% of ambiguity fixed solutions have positioning errors smaller than 3 cm.

Keywords Multi-dimensional particle filter approach · multi-GNSS integration · Ambiguity resolution · Inter-system bias estimation

1 Introduction

The integration of multi-GNSS outperforms individual system in accuracy, reliability and availability (Force and Miller 2013; Li et al. 2015; Odolinski et al. 2014). In traditional integration, only intra-system double difference (DD) algorithm is adopted to resolve integer DD ambiguities because of their signal consistence (Dach, et al., 2009; Ineichen et al. 2008). Actually, inter-system DD integer ambiguities can also be resolved as long as inter-system biases (ISB) are known (Odijk and Teunissen 2013a, 2013b; Paziewski and Wielgosz 2015; Odolinski et al. 2014; Julien et al. 2003; Tian et al. 2016). Thus multi-GNSS precise relative positioning can be achieved. The resolution of inter-system DD integer ambiguities is very meaningful as more and more new systems, such as European Galileo system, Chinese BeiDou navigation satellite system (BDS), Japanese Quasi-Zenith Satellite System (QZSS) and the Indian NAVigation with Indian Constellation (NAVIC), are under rapid development. It is particularly important under certain poor observing environments where signals of some satellites may have been blocked. In such a situation, there probably are not sufficient satellite signals from an individual system to perform position fixing. Thus the use of multi-system GNSS signals becomes an absolute necessity in order to fix the ambiguities reliably.

The ISB in multi-GNSS integration is caused by the hardware delays (Odijk and Teunissen 2013a) or say the uncalibrated phase delay (Ge et al. 2008). The phase ISB can be divided into two parts, one part that is a multiple of full wavelength and the remaining part that is a fraction of a full wavelength. The remaining part is called fractional ISB (F-ISB). The former part lumps into the DD integer ambiguities and does not affect the ambiguity resolution. However, the latter one, if not corrected, destroys the integer nature of the ambiguities, leading to failure of ambiguity fixing. Thus, only the F-ISB needs to be accurately estimated and removed.

In order to obtain accurate phase F-ISB, several estimation methods have been proposed. Odijk and Teunissen (2013a) added the F-ISB parameter into the inter-system DD-model to preserve the integer nature of the inter-system DD-ambiguities. The sum of the inter-system DD-ambiguity and F-ISB in one of the DD-phase equations is regarded as one parameter and thus the inter-system DD-ambiguity will not be fixed in F-ISB estimation. Paziewski and Wielgosz (2015) determined the ISB parameter by introducing an initial constraint on the F-ISB parameter, zero mean Gaussian noise with a standard deviation (STD) of 0.5 cycle of signal wavelength. It is obvious that the inter-system ambiguity fixing can degrade the final ambiguity fixing performance once the true F-ISB value is far from zero. In general, these traditional methods try to estimate F-ISB through parameterization in the DD-observation equations. Thus, integer ambiguity resolution cannot be conducted before the F-ISB is precisely known, because of the rank-deficiency caused by the F-ISB and the float ambiguity parameters (Odijk and Teunissen 2013a). On the other hand, the F-ISB parameter can be precisely determined after the intra-system DD-ambiguities are successfully fixed to integers. Nevertheless, the intra-system DD-ambiguity cannot always be fixed reliably. Under some challenging observation conditions, such as in urban canopy areas where signals could be easily blocked or interrupted, only a small number of satellites can be observed from each system. In such a case, the fixing of intra-system DD-ambiguity is a challenge. Subsequently the F-ISB cannot be precisely estimated if the traditional estimation strategy is used. Consequently, the fixing of inter-system DD-ambiguities is not possible. Therefore, a new estimation method that can simultaneously estimate the F-ISB and fix the inter-system DD-ambiguities is needed.

Tian et al. (2015) developed a particle-filter-based method to estimate the inter-frequency bias (IFB) rate in GLONASS data processing and this method has also been adapted for ISB estimation (Tian et al. 2016). Particle filter is proposed by Gordon et al (1993) and can be regarded as the Bayesian filtering implemented via Monte Carlo method. The particle filter represents the PDF of variables by a number of particle values instead of by only the mean value in Kalman filter. This kind of filter is able to solve non-Gaussian and non-linear state space problems and has been widely used in various applications, such as digital data processing, target tracking, terrestrial navigation, indoor navigation (Doucet et al 2001; Gustafsson et al 2002).

The particle filter based ISB estimation approach takes advantage of the integer nature of the ambiguities via the ambiguity-fixing RATIO which was proposed by Euler and Schaffrin (1991) indicating the closeness between the ambiguity's float solution and the nearest integer vector (Verhagen and Teunissen 2013). In this approach, the F-ISB samples are first generated and then treated as known F-ISB values in DD-ambiguity resolution. The F-ISB samples that have the closest values to the truth can recover the integer nature of the inter-system DD-ambiguities and result in the largest RATIO values. After the particle weights are updated according to the RATIO values in the particle filtering, the F-ISB can be successfully estimated according to the weighted particles. Because the estimated F-ISB samples are treated as knowns, both intra- and inter-system DD-ambiguities can be fixed simultaneously (Tian et al. 2016). This method estimates the float DD-ambiguities with the model of employing an a priori ISB value as described in (Paziewski and Wielgosz 2015), thus the singularity caused by the rank-deficiency is solved. At the same time, when the F-ISB are held as known values, the inter-system DD-ambiguity resolution algorithm has the same form of the intra-system one. This is convenient for computer program implementation. In addition, the observation model is strengthened, which benefits the final positioning solution (Khodabandeh and Teunissen, 2016).

However, this particle-filter approach developed in Tian et al. (2016) is a one-dimensional method, which is suitable for estimating one ISB parameter when two GNSS systems are integrated. To apply this method to the integration of more GNSS systems, multi-dimensional algorithm is required. A method for multi-GNSS system integration is apparently needed as more and more GNSS systems are in rapid development. In this paper, we will investigate the multi-dimensional (multivariate) particle-filter approach for multiple-ISB estimation. We will show the performance of this method through examples of satellites from three GNSS systems. In one challenging observation condition when only two satellites from each of three systems are observed, totally two F-ISB parameters need to be estimated and five DD-ambiguities need to be fixed. DD-ambiguity integer resolution is not possible using traditional intra-system DD-model. Our new method shows that successful ambiguity fixing and accurate F-ISB estimation can be achieved simultaneously.

In the multi-dimensional estimation, the likelihood function of the measurements is usually determined as the product of the likelihood function of each individual measurement

(Candy 2009; Haug 2012). The one-dimensional RATIO-derived likelihood function has been proposed in Tian et al. (2016). However, using the product of these likelihood functions as the likelihood function of multi-dimensional estimation is not a good choice. This is because the one-dimensional likelihood function can be unreliable when the number of satellites from two GNSS systems is too small. In this case, we will show that the multi-dimensional likelihood function can be designed with RATIO directly and RATIO can represent the quality of multi-dimensional F-ISB samples. With the multi-dimensional particle-filter approach, multiple F-ISB parameters can be estimated simultaneously.

In the following, we first present the intra- and inter-system DD-observable models in section 2 and describe the multi-dimensional particle-filter approach in section 3. The relationship between RATIO distribution and different F-ISB values are investigated with examples in section 4. The estimated results and the discussion are presented in section 5 and section 6, respectively. The conclusions are given in the section 7.

2 GNSS Observation Equations

The GNSS code pseudorange and carrier phase observation equations can be expressed as below (Teunissen 1996).

$$P_a^{s_1,i} = \rho_a^{s_1,i} - c\left(\delta t_a - \delta t^{s_1,i}\right) + d_a^{s_1,i} - d^{s_1,i} + I_a^{s_1,i} + T_a^{s_1,i}$$

$$+R_a^{s_1,i} + S_a^{s_1,i} + M_a^{s_1,i} + \varepsilon_a^{s_1,i}\ , \tag{1a}$$

$$\lambda^{s_1,i}\Phi_a^{s_1,i} = \rho_a^{s_1,i} - c\left(\delta t_a - \delta t^{s_1,i}\right) + \mu_a^{s_1,i} - \mu^{s_1,i} + \lambda^{s_1,i}N_a^{s_1,i} + \lambda^{s_1,i}\psi_a^{s_1,i} - I_a^{s_1,i} + T_a^{s_1,i} +$$

$$R_a^{s_1,i} + S_a^{s_1,i} + m_a^{s_1,i} + \xi_a^{s_1,i}. \tag{1b}$$

where P is the code pseudorange measurement; i and a are indices for GNSS satellite and receiver, respectively; s_1 refers to the name of a particular GNSS constellation system; ρ is the distance between satellite i and receiver a; δt_a and $\delta t^{s_1,i}$ are the receiver and satellite clock biases, respectively. $d_a^{s_1,i}$ and $d^{s_1,i}$ are the receiver and satellite hardware delays, respectively, in code observations; I is the ionospheric delay; T the tropospheric delay; R is the effect of the relativity; S is the Sagnac effect i.e. earth rotation correction; M refers to the multipath effect on the code pseudorange measurement; ε denotes the remaining errors which are considered as white noise; Φ is the carrier phase measurement; λ is the wavelength; $\mu_a^{s_1,i}$ and $\mu^{s_1,i}$ are the receiver and satellite hardware delays, respectively, in carrier phase measurement; N is the phase ambiguity which is an integer number; ψ is the initial phase value; m refers to the multipath effects; ξ is the noise on carrier phase observation.

DD models between receivers and satellites can eliminate or largely reduce the errors, such as the receiver and satellite clock offsets, the atmosphere delays. In the inter-system DD models, the receiver clock biases are eliminated because the signals of different systems are received at the same time as they share the same receiver reference clock (Melgard et al. 2013). The satellite hardware delays are eliminated by between-receiver differencing. The relativity effects and the Sagnac effects can be accurately calculated. Although the multipath effect can hardly be eliminated in the data processing as they depend on the observation environments, they can be mitigated through some antenna and receiver mitigation techniques. In addition, multipath can be reduced by setting a relatively higher elevation mask and setting at a station with good visibility. Thus the multipath effects are neglected in this investigation.

However, the receiver hardware delays cannot be cancelled due to different paths for signals from different satellite systems (Kozlov and Tkachenko 1997; Wang 2001). The delays in digital signal processing may also be different and can be regarded as part of the hardware delays, so is the initial phase term in the carrier phase observation. The between-receiver hardware delays lead to the ISB, which must be estimated in the data processing in order to fix the inter-system DD-ambiguities to integers. If the estimated float DD-ambiguities can be successfully fixed to integers, the positioning results can be significantly improved (Blewitt 1989; Dong and Bock 1989). For intra-system DD-observations, i.e. within the same single GNSS system, many methods have been developed to fix DD-ambiguities to integer values. For inter-system DD-observations, i.e. between different GNSS systems, their DD-ambiguities can also be fixed to integers, as long as the inter-system bias (ISB) is known.

Based on the above discussion and considering that satellites from different systems have different signal frequencies, the generalized DD-observation equations can be written as,

$$P_{ab}^{s_1s_2,ij} = \rho_{ab}^{s_1s_2,ij} + d_{ab}^{s_1s_2,ij} + I_{ab}^{s_1s_2,ij} + T_{ab}^{s_1s_2,ij} + \varepsilon_{ab}^{s_1s_2,ij}, \tag{2a}$$

$$\lambda^{s_2,j}\Phi_{ab}^{s_2,j} - \lambda^{s_1,i}\Phi_{ab}^{s_1,i} = \rho_{ab}^{s_1 s_2,ij} + \mu_{ab}^{s_1 s_2,ij} + \lambda^{s_2,j}N_{ab}^{s_2,j} - \lambda^{s_1,i}N_{ab}^{s_1,i} - I_{ab}^{s_1 s_2,ij} + T_{ab}^{s_1 s_2,ij} + \xi_{ab}^{s_1 s_2,ij}. \quad (2b)$$

where s_1 and s_2 are the systems to which the satellites i and j belong, respectively; $d_{ab}^{s_1 s_2,ij}$ and $\mu_{ab}^{s_1 s_2,ij}$ are DD hardware delays for pseudorange and carrier phase observations, respectively. If s_1 and s_2 are from the same system and it is a CDMA system, the $d_{ab}^{s_1 s_2,ij}$ and $\mu_{ab}^{s_1 s_2,ij}$ have a value of zero. If s_1 and s_2 are from different CDMA systems, $d_{ab}^{s_1 s_2,ij}$ and $\mu_{ab}^{s_1 s_2,ij}$ may have non-zero values but their values are the same for different satellites. If s_1 and s_2 are GLONASS FDMA system, then $d_{ab}^{s_1 s_2,ij}$ and $\mu_{ab}^{s_1 s_2,ij}$ may have non-zero values; their values are different for different GLONASS FDMA satellites due to the existence of GLONASS IFB.

Inter-System DD-Model with the Same Frequency

When GNSS signals from different systems have the same frequency, DD-ambiguities can be formed because they have the same wavelength. Their hardware delays however may not be eliminated (Odijk and Teunissen 2013a) and it is referred to as ISB in the follows. The DD observation model can be expressed by:

$$P_{ab}^{s_1 s_2,ij} = \rho_{ab}^{s_1 s_2,ij} + d_{ab}^{s_1 s_2} + I_{ab}^{s_1 s_2,ij} + T_{ab}^{s_1 s_2,ij} + \varepsilon_{ab}^{s_1 s_2,ij}, \quad (3a)$$

$$\lambda^{s_1 s_2,ij}\Phi_{ab}^{s_1 s_2,ij} = \rho_{ab}^{s_1 s_2,ij} + \mu_{ab}^{s_1 s_2} + \lambda^{s_1 s_2,ij}N_{ab}^{s_1 s_2,ij} - I_{ab}^{s_1 s_2,ij} + T_{ab}^{s_1 s_2,ij} + \xi_{ab}^{s_1 s_2,ij}. \quad (3b)$$

The pseudorange ISB $d_{ab}^{s_1 s_2}$ can be directly determined using the pseudorange observations with model (2a), but it is not the case for carrier phase ISB $\mu_{ab}^{s_1 s_2}$. As aforesaid, the carrier phase ISB can be expressed by its integer and fractional parts as:

$$\mu_{ab}^{s_1 s_2} = \tilde{\mu}_{ab}^{s_1 s_2} + \lambda N_{\tilde{\mu}}^{s_1 s_2} \quad (4)$$

where $\tilde{\mu}_{ab}^{s_1 s_2}$ is the F-ISB, $N_{\tilde{\mu}}^{s_1 s_2}$ is an integer; λ is the common wavelength. The integer part $N_{\tilde{\mu}}^{s_1 s_2}$ lumps into the integer DD-ambiguity $N_{ab}^{s_1 s_2,ij}$ and does not impose an impact on ambiguity fixing. However the F-ISB $\tilde{\mu}_{ab}^{s_1 s_2}$ destroys the integer nature of DD-ambiguities and it needs to be estimated in order to fix DD-ambiguities to integer.

Inter-System DD-Model with Narrowly Spaced Frequencies

In the inter-system model, when GNSS signals have different frequencies, the DD-ambiguities cannot be formed. The hardware delays may not be eliminated either. Thus, the inter-system DD-model of different frequencies is:

$$P_{ab}^{s_1s_2,ij} = \rho_{ab}^{s_1s_2,ij} + d_{ab}^{s_1s_2} + I_{ab}^{s_1s_2,ij} + T_{ab}^{s_1s_2,ij} + \varepsilon_{ab}^{s_1s_2,ij}, \tag{5a}$$

$$\lambda^{s_2,j}\Phi_{ab}^{s_2,j} - \lambda^{s_1,i}\Phi_{ab}^{s_1,i} = \rho_{ab}^{s_1s_2,ij} + \mu_{ab}^{s_1s_2} + \lambda^{s_2,j}N_{ab}^{s_2,j} - \lambda^{s_1,i}N_{ab}^{s_1,i} - I_{ab}^{s_1s_2,ij} + T_{ab}^{s_1s_2,ij} + \xi_{ab}^{s_1s_2,ij}. \tag{5b}$$

The pseudorange ISB $d_{ab}^{s_1s_2}$ can still be directly determined using the pseudorange observations with model (5a). The phase ISB $\mu_{ab}^{s_1s_2}$ can be rewritten as the sum of three parts: an approximate ISB value, the integer part of the remaining ISB, and an accurate F-ISB of the remaining ISB value (Tian et al. 2017). The approximate ISB value can be considered equal to the pseudorange ISB, while the F-ISB needs to be estimated accurately. Thus the phase ISB can be expressed by:

$$\mu_{ab}^{s_1s_2} = \tilde{\mu}_{ab}^{s_1s_2} + d_{ab}^{s_1s_2} + \bar{\lambda}N_{\tilde{\mu}_{ab}^{s_1s_2}} \tag{6}$$

where $\tilde{\mu}_{ab}^{s_1s_2}$ is the F-ISB; $d_{ab}^{s_1s_2}$ is the approximate ISB; $\bar{\lambda}N_{\tilde{\mu}_{ab}^{s_1s_2}}$ is the integer part of ISB with integer $N_{\tilde{\mu}_{ab}^{s_1s_2}}$; $\bar{\lambda}$ is the wavelength corresponding to $N_{\tilde{\mu}_{ab}^{s_1s_2}}$. After the approximate ISB $d_{ab}^{s_1s_2}$ is determined and removed, the integer $N_{\tilde{\mu}_{ab}^{s_1s_2}}$ is a small value and can be lumped into the inter-system DD integer ambiguities and its effect on DD-ambiguity estimation is negligible. Thus, if $\tilde{\mu}_{ab}^{s_1s_2}$ is accurately estimated, the integer DD-ambiguities can be successfully determined.

Integration of More Than Two Systems

When more than two GNSS systems are integrated for positioning and navigation, multiple F-ISB values need to be estimated. Those F-ISB parameters may include the ones between the same frequencies and between different frequencies, but they can be estimated by the same procedure.

Usually, there is only one independent ISB parameter for every two systems. Therefore, for a combination of M systems, the number of independent ISB or F-ISB parameters will be $(M-1)$. All the F-ISB parameters can be estimated via the multi-dimensional particle-filter approach. In this approach, the inter-system DD-ambiguities are well utilized and the reliability of F-ISB estimation is improved especially under poor observation conditions with limited number of satellites.

3 Multi-dimensional Particle Filter Approach

For a random state vector $\boldsymbol{x} = \left[x_1, x_2, \dots, x_{n_x}\right]^T$, if its probability density function (PDF) is $p(\boldsymbol{x})$, the expectation of $\boldsymbol{x}$ can be expressed as $\hat{\boldsymbol{x}} = \int_{-\infty}^{+\infty} \boldsymbol{x} p(\boldsymbol{x}) d\boldsymbol{x}$ (Gustafsson et al 2002, Haug 2012). Assume at epoch k the posterior PDF of $\boldsymbol{x}_k$ is $p(\boldsymbol{x}_k|\boldsymbol{y}_{1:k})$ and there is a priori PDF of $\boldsymbol{x}_k$ expressed by $q(\boldsymbol{x}_k|\boldsymbol{y}_{1:k})$ from which samples can be generated, the expectation of $\boldsymbol{x}_k$ can be calculated by:

$$\hat{\boldsymbol{x}}_{\boldsymbol{k}} = \int \boldsymbol{x}_{\boldsymbol{k}} \frac{p(\boldsymbol{x}_k|\boldsymbol{y}_{1:k})}{q(\boldsymbol{x}_k|\boldsymbol{y}_{1:k})} q(\boldsymbol{x}_k|\boldsymbol{y}_{1:k}) d\boldsymbol{x}_k = \int \boldsymbol{x}_k \, w(\boldsymbol{x}_k) \, q(\boldsymbol{x}_k|\boldsymbol{y}_{1:k}) d\boldsymbol{x}_k \tag{7}$$

where $w(x_k) = \frac{p(x_k|y_{1:k})}{q(x_k|y_{1:k})}$ can be regarded as a weight; $\boldsymbol{y}_{1:k} = [\boldsymbol{y}_1, \boldsymbol{y}_2, \cdots \boldsymbol{y}_k]^T$ is the vector of all the measurements from epoch 1 to epoch k. The estimation process is assumed to be a first-order Markov process which means the estimated state vector at epoch k is only related to the solution at the last epoch $(k-1)$ and not solutions of previous epochs such as $\boldsymbol{x}_{k-2}, \dots, \boldsymbol{x}_0$. If the previous epoch samples $\left\{\boldsymbol{x}_{k-1}^i\right\}_{i=1}^N$ at epoch (k-1) are generated from $q(\boldsymbol{x}_{k-1}|\boldsymbol{y}_{1:k-1})$, from Bayes's theorem the weight $w(\boldsymbol{x}_k)$ can be expressed by

$$w(\boldsymbol{x}_k) \propto \sum_{i=1}^N w_{k-1}^i \frac{p\left(\boldsymbol{y}_k|\boldsymbol{x}_k\right) p\left(x_k|x_{k-1}^i\right)}{q\left(x_k|x_{k-1}^i, y_k\right)} \tag{8}$$

where $\propto$ indicates direct proportionality; $p(\boldsymbol{y}_k|\boldsymbol{x}_k)$ is the likehood function of $\boldsymbol{y}_k$ given $\boldsymbol{x}_k$; w_{k-1}^i is the weight of particle i in k-1 epoch. Details of the derivation of Eq. (8) can be found in (Doucet et al 2001; Arulampalam 2002; Haug 2012). The PDF $q\left(\boldsymbol{x}_k|\boldsymbol{x}_{k-1}^i, \boldsymbol{y}_k\right)$ is supposed to be calculated according to $q(\boldsymbol{x}_{k-1}|\boldsymbol{y}_{1:k-1})$ and the prediction model of the filtering. In practice, usually let $q(\boldsymbol{x}_k|\boldsymbol{x}_{k-1}, \boldsymbol{y}_k) = p(\boldsymbol{x}_k|\boldsymbol{x}_{k-1})$ (Gordon et al 1993) and then the weights of particles for each epoch can be updated by:

$$w_k^i = w_{k-1}^i p\left(\boldsymbol{y}_k|\boldsymbol{x}_k^i\right) \tag{9}$$

After the weights are updated, expectation of the state vector and the STD of the particles can be calculated by:

$$\widehat{\boldsymbol{x}}_k \approx \sum_{i=1}^{N} \boldsymbol{x}_k^i \, w_k^i \tag{10}$$

$$\mathrm{var}(\widehat{\boldsymbol{x}}_k) \approx \sum_{i=1}^{N} (\boldsymbol{x}_k^i - \widehat{\boldsymbol{x}}_k)\,(\boldsymbol{x}_k^i - \widehat{\boldsymbol{x}}_k)^T w_k^i \tag{11}$$

Obviously, $p(\boldsymbol{y}_k|\boldsymbol{x}_k)$ is important to the estimation of the state vector.

Assume there are more than one independent unknown parameter included in the state vector, the same number of independent measurements or even more are needed so that the solution of the unknown parameters in the state vector can be well constrained. In this case, $\boldsymbol{y}_k$ can be expressed as $\boldsymbol{y}_k = \left[y_1, y_2, \cdots, y_{L_k}\right]^T$, where L_k is the number of measurements at epoch k.

The likelihood function of the independent measurements $p(\boldsymbol{y}_k|\boldsymbol{x}_k)$ can be expressed as a joint density (Candy 2009; Haug 2012) and calculated by:

$$p(\boldsymbol{y}_k|\boldsymbol{x}_k) = \prod_{h=1}^{h=L_k} p\left(y_h|\boldsymbol{x}_k\right), \tag{12}$$

where $p(y_h|\boldsymbol{x})$ is the likelihood function of the observation y_h given $\boldsymbol{x}$.

In GNSS data processing, if we assume that F-ISB parameters are elements in the state vector $\boldsymbol{x}$ and that the GNSS observations are elements of $\boldsymbol{y}_k$, we cannot get the likelihood function of $\boldsymbol{y}_k$ given F-ISB vector $\boldsymbol{x}$. This is because of the rank-deficiency caused by F-ISB and float ambiguity parameters. Those parameters are distinguishable only after one of the two kinds is accurately determined, such as the integer ambiguities are successfully resolved.

A designed one-dimensional likelihood function has been proposed by Tian et al. (2016) based on RATIO to estimate one ISB parameter. It is likely to calculate the multi-dimensional function from the product of the one-dimensional functions. But the model to calculate the RATIO values for one-dimensional likelihood function will be weak when the number of satellites from each system is small, because the one-dimensional likelihood function utilizes only one inter-system DD-ambiguity in the F-ISB estimation. However, we will show that for multi-dimensional F-ISB estimation, the likelihood function can be directly designed via RATIO values with multiple F-ISB parameters and can fix all inter-system DD-ambiguities.

In this approach, the samples representing multi-dimensional F-ISB values are first generated. Those samples are set as known F-ISB values. Thus, integer candidates of all inter- and intra-system DD-ambiguities can be estimated using the LAMBDA method (Khodabandeh and Teunissen 2016; Kubo et al. 2018). Afterwards, the corresponding RATIO values are calculated and utilized to determine the values of the multi-dimensional likelihood functions, which is a function of all unknown F-ISB parameters and can be seen as the likelihood function of the ambiguities being fixed with given F-ISBs. Obviously, the values of this function depend on more than one F-ISB parameters. The weight updates can be expressed as:

$$w_k^i = w_{k-1}^i p\left(\breve{\boldsymbol{b}}_k | \left(\mu_k^{s_1 s_2}, \mu_k^{s_1 s_3}, \cdots \mu_k^{s_1 s_M}\right)^i\right) \tag{13}$$

with

$$p\left(\breve{\boldsymbol{b}}_k | \left(\mu_k^{s_1 s_2}, \mu_k^{s_1 s_3}, \cdots \mu_k^{s_1 s_M}\right)^i\right) = \frac{RATIO\left(\left(\mu_k^{s_1 s_2}, \mu_k^{s_1 s_3}, \cdots \mu_k^{s_1 s_M}\right)^i\right)}{\sum_{i=1}^{N} RATIO\left(\left(\mu_k^{s_1 s_2}, \mu_k^{s_1 s_3}, \cdots \mu_k^{s_1 s_M}\right)^i\right)}, \tag{14}$$

where state vector $\breve{\boldsymbol{b}}_k$ refers to the correct integer ambiguity vector at epoch k; M is the number of systems; N is the number of samples (i.e. particles). This equation can be employed to estimate all F-ISB parameters at the same time.

Besides, the prediction models of the F-ISB variables can be expressed by:

$${\mu_{ab}}_k^{s_1 s_m} = {\mu_{ab}}_{k-1}^{s_1 s_m} + \epsilon_{\mu_{ab}^{s_1 s_m}}, \tag{15}$$

where $\epsilon_{\mu_{ab}^{s_1 s_m}}$ is assumed to be white noise; $m = 2 \ldots, M$ refers to satellite system. The procedure for the multi-dimensional F-ISB estimation is given below:

Step 1: Process the phase and code pseudorange measurements according to the models to get the normal equation. It is assumed that the observed satellites from M systems have the same or narrowly-spaced frequency band and have $(M-1)$ F-ISB parameters.

Step 2: Before the first epoch, initial particles are obtained by sampling randomly over the interval with breadth of one wavelength. As the number of F-ISB is $(M-1)$, each particle has $(M-1)$ F-ISB values i.e. $(M-1)$ dimensions. If the number of particles for each dimension (i.e. each F-ISB parameter) is denoted by N_0, totally ${N_0}^{M-1}$ combinations can be generated leading to $N = {N_0}^{M-1}$ particles. Each particle is assigned the initial weight value $1/N$. Therefore, the generated particle collection can be represented by $\boldsymbol{x}_0 = \left\{\left\{x_0^{i,j}\right\}_{j=1}^{M-1}, 1/N\right\}_{i=1}^{N_0}$. For other epochs $k = 1,2 \ldots$, the particle collection can be expressed as $\boldsymbol{x}_k = \left\{\left\{x_k^{i,j}\right\}_{j=1}^{M-1}, w_k^i\right\}_{i=1}^{N_k}$ with w_k^i from the last epoch $(k - 1)$.

Step 3: For each particle, the $(M-1)$ values are set as known F-ISB. The float ambiguities and the associated variance-covariance matrices are calculated. The LAMBDA method is then employed to obtain the integer ambiguity candidates and the corresponding RATIO values are calculated by

$$RATIO = \frac{(\hat{\boldsymbol{b}} - \breve{\boldsymbol{b}}')^T \boldsymbol{Q}_{\hat{\boldsymbol{b}}\hat{\boldsymbol{b}}} (\hat{\boldsymbol{b}} - \breve{\boldsymbol{b}}')}{(\hat{\boldsymbol{b}} - \breve{\boldsymbol{b}})^T \boldsymbol{Q}_{\hat{\boldsymbol{b}}\hat{\boldsymbol{b}}} (\hat{\boldsymbol{b}} - \breve{\boldsymbol{b}})} \tag{16}$$

where $\hat{\boldsymbol{b}}$ refers to the estimated float DD-ambiguity vector; $\boldsymbol{Q}_{\hat{\boldsymbol{b}}\hat{\boldsymbol{b}}}$ is the variance-covariance matrix of $\hat{\boldsymbol{b}}$; $\breve{\boldsymbol{b}}$ indicates the primary candidate of the DD integer ambiguity vector; $\breve{\boldsymbol{b}}'$ indicates the secondary candidate of the DD integer ambiguity vector for minimizing $f(\boldsymbol{b}) = (\hat{\boldsymbol{b}} - \boldsymbol{b})^T \boldsymbol{Q}_{\hat{\boldsymbol{b}}\hat{\boldsymbol{b}}} (\hat{\boldsymbol{b}} - \boldsymbol{b})$.

Step 4: Normalize the RATIO values according to Eq. (). Update the weights with the normalized RATIO. Calculate the estimated F-ISB and their variances of the particles by Eq. (10) and (11), respectively.

Step 5: If the STD of the estimated F-ISB is larger than a predefined threshold, use the cluster analysis method to determine whether the particles have been divided into more than one group, and shift them into one group if yes.

In detail, following steps are implemented for each dimension of the particle values:

(1) Find two particles with the largest distance as the first particles of each group.

(2) Cluster other particles according to their distances to the first particles.

(3) Calculate the centroid of each group. If the distance of the two centroids is close to one wavelength of the carrier phase, shift the cluster with larger absolute centroid value to the cluster with smaller absolute centroid value by plus or minus one wavelength.

.

Step 6: Resample the particles if the following is satisfied

$$N_{eff} < N_{th} , \tag{17}$$

where N_{eff} is the effective number of samples while the threshold N_{th} can be set as two thirds of N. N_{eff} is calculated as:

$$N_{eff} = \frac{1}{\sum_{i=0}^{N} \left(w_k^i\right)^2}, \tag{18}$$

Step 7: Predict the particles for the next epoch according to the prediction model Eq. (15).

Step 8: Repeat steps 1 to 7 for the next epoch.

This method will be implemented in an example of a two-dimensional case, where its advantages will be demonstrated.

4 RATIO distribution with two F-ISB parameters

The RATIO value is a function of (M-1) F-ISB parameters. We investigate the relationship between RATIO and multi-F-ISB parameters in multi-system integration using three examples, e.g. (1) GPS L5-Galileo E5a and GPS L5-QZSS L5, (2) GPS L1-Galileo E1 and GPS L5-Galileo E5a, and (3) GPS L1-Galileo E1 and GPS L1-BDS B1. For the sake of convenience, we denote the above three examples as GEJ_L5, GE_L1L5 and GEB_L1, respectively. In each of the three examples, two F-ISB parameters need to be estimated.

Data

First, the GEJ_L5 integration is investigated with a zero-baseline SIN0-SIN1 dataset collected on the day of year (DOY) 007 in 2016. The SIN0 station is equipped with a JAVAD TRE_G3TH DELTA receiver and the SIN1 is installed with a TRIMBLE NETR9 receiver. The satellite numbers for GPS L5, Galileo E5a and QZSS L5 are shown in Fig. 1(a).

The data employed for the investigation of GE_L1L5 are from a 1266 m long baseline TLSG-TLSE which could provide GPS L1, L5 and Galileo E1, E5a observations. The data were collected on DOY 007 of 2016 at IGS stations TLSG and TLSE equipped with LEICA GRX1200GGPRO and TRIMBLE NETR9 receivers, respectively. The numbers of satellites for

GPS L1 and Galileo E1 are shown in the Fig. 1(b), while these for GPS L5 and Galileo E5a are displayed in Fig. 1(c).

The data of baseline TLSG-TLSE were collected on DOY 001 of 2015 to investigate the integration of GEB_L1. The two stations are equipped with the same receivers as the GE_L1L5 integration. The numbers of satellites for GPS L1, Galileo E1 and BDS B1 are depicted in Fig. 1(d).

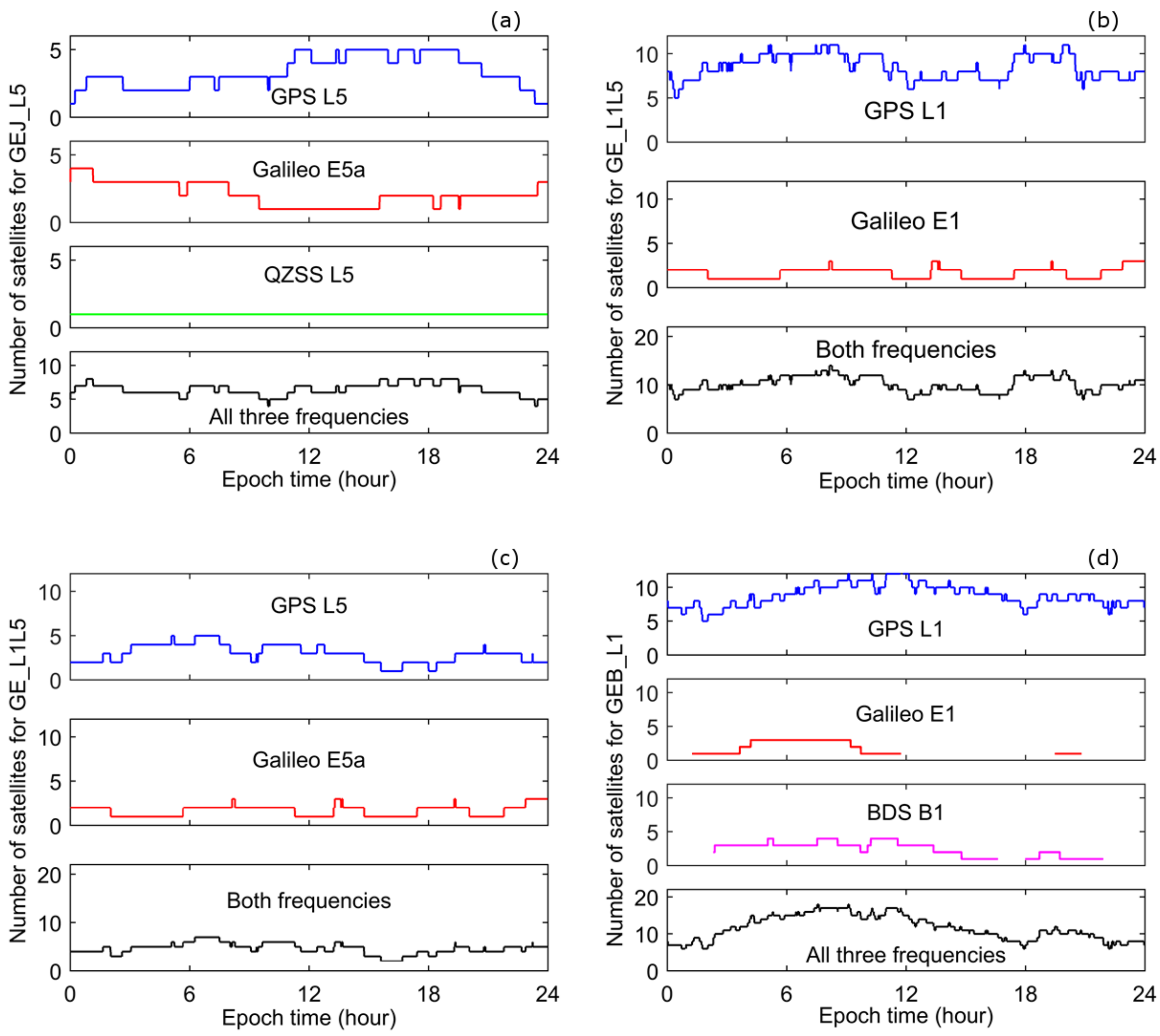

Fig. 1 Numbers of satellites in GEJ_L5 integration for baseline SIN0-SIN1 on DOY 007 of 2016(a). Numbers of satellites in GE_L1, GE_L5 integration for baseline TLSG-TLSE on DOY 007 of 2016 (b and c, respectively), as well as numbers of satellites in GEB_L1 integration for baseline TLSG-TLSE on DOY 001 of 2015 (d).

RATIO distribution with two F-ISB parameters To evaluate the RATIO distribution after the F-ISB values, the initial interval [-0.2, 0.2] m, the breadth of which is about twice wavelength of GNSS signals, is evenly sampled 40 times with the sampling interval of 0.01 m. Since three GNSS systems are used, two F-ISB parameters need to be estimated. It should be noted in some combinations (e.g. GPS L1-Galileo E1, GPS L5-Galileo E5a), only two systems are involved but there are two F-ISB parameters too, because each frequency combination has an F-ISB parameter and two frequency combinations are employed. In our three integration cases, two F-ISB parameters are involved. Consequently, a total of 1600 F-ISB sample combinations (40x40) can be generated. Corresponding1600 RATIO are calculated for each epoch. The RATIO distributions of three epochs for the above three data sets are shown in Fig. 2.

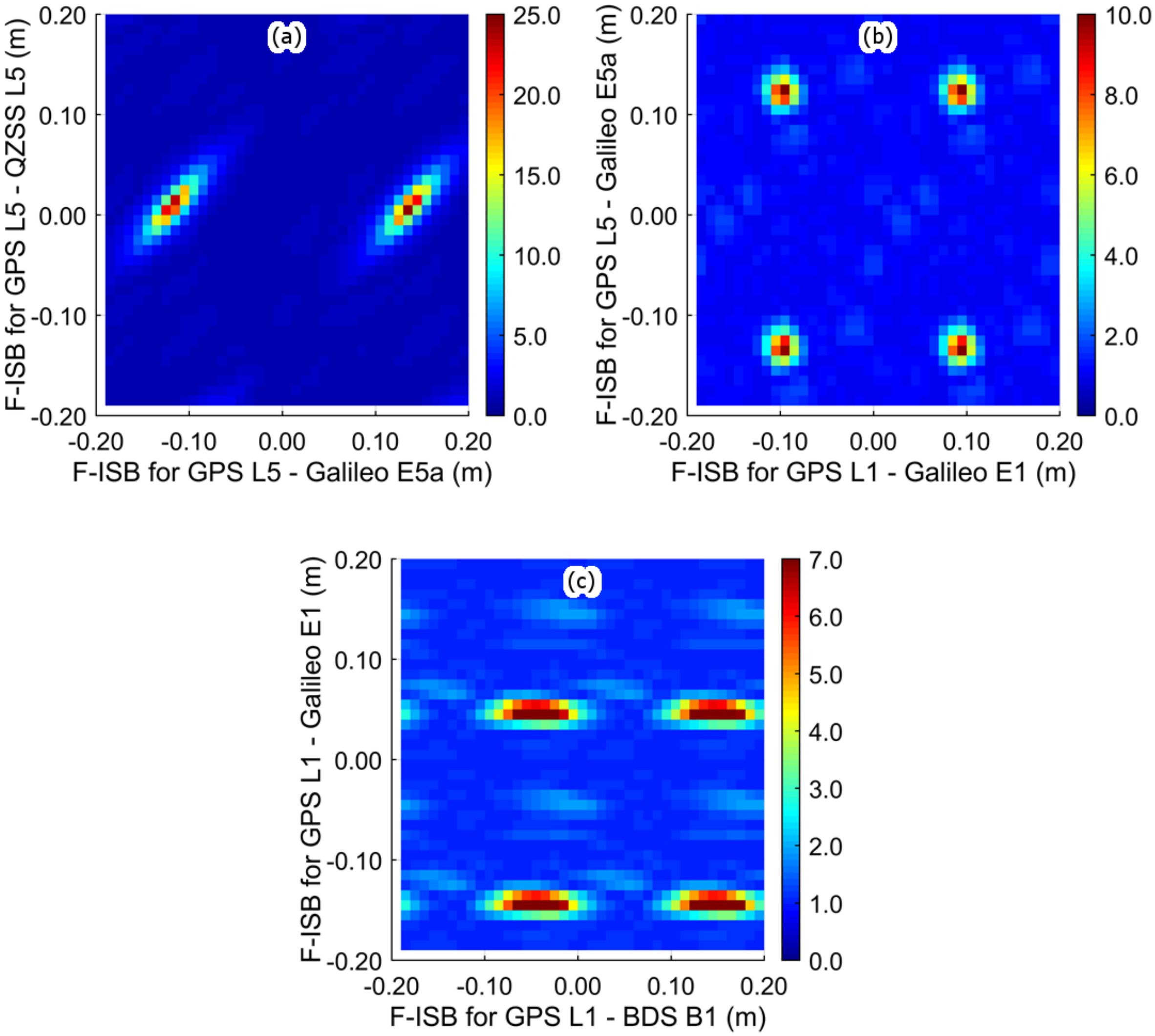

Fig. 2 RATIO distribution in the integration of GEJ_L5 for baseline SIN0-SIN1 at epoch 0:00:00 on DOY 007 of 2016 (a); RATIO distribution in the integration of GE_L1L5 for baseline TLSG-TLSE at epoch 0:02:30 on DOY 007 of 2016 (b); RATIO distribution in the integration of GEB_L1 for baseline TLSG-TLSE at epoch 3:39:00 on DOY 001 of 2015 (c). The color bar shows the different RATIO values.

For the first integration GEJ_L5 for baseline SIN0-SIN1, the RATIO at epoch 0:00:00 on DOY 007 of 2016 is displayed. The RATIO distribution corresponding to each combination of sampled values of the two F-ISB parameters, one for GPS L5 and Galileo E5a integration and the other one for GPS L5 and QZSS L5 integration, is shown in Fig. 2(a). The second case is the integration of GE_L1L5 for baseline TLSG-TLSE at epoch 0:02:30 on DOY 007 of 2016. The RATIO distribution with two F-ISB parameters, one for GPS L1 and Galileo E1 integration and the other one for GPS L5 and Galileo E5a integration, is shown in Fig. 2(b). The third one is the integration of GEB_L1 for baseline TLSG-TLSE at epoch 3:39:00 on DOY 001 of 2015. The RATIO distribution with two F-ISB parameters, one for GPS L1 and Galileo E1 integration and the other one for GPS L1 and BDS B1 integration, is depicted in Fig. 2(c).

In Fig. 2(a), the 0.4 m×0.4 m area shows us the RATIO distribution, where two maximum values are highlighted on the blue background. Those maximum values have different abscissas but their ordinates are similar. In the GEJ_L5 integration, the wavelength for this frequency band is 0.2548 m. The F-ISB for GPS L5 and QZSS L5 has a value near zero and thus only one maximum RATIO value can be observed over the interval [-0.2, 0.2] m. The F-ISB for GPS L5 and Galileo E5a has a value near half cycle, thus two maximum RATIO values can be observed in the same interval. In the Fig. 2 (b), the F-ISB value for GPS L5 and Galileo E5a integration, as well as the value for GPS L1 and Galileo E1 integration, is near half a cycle. Thus, four maximum values can be observed. In Fig. 2(c), the wavelengths for both frequencies are smaller than 0.2 m and four local maximum RATIO values can be observed regardless of the F-ISB true values.

When the number of observed satellites is small, the ambiguity fixing is not reliable. In this case, the local maximum values in the RATIO distribution may scatter at different places, but these local maximum values can still be large. For example, for the case (3) dataset, we employ only 3 GPS, 2 Galileo and 3 BDS satellites at epoch GPS time 3:39:00 on DOY 001 of 2015. The RATIO distribution is calculated and presented in Fig. 3 below and four large local maximum RATIO values can be observed. The dataset in Fig. 3 is the same as that in Fig. 2c with only difference on the number of observed satellites. Apparently, the distribution of maximum values is not the same as that in Fig. 2(c). The 4 local maximum RATIO values in Fig. 3 correspond to four pairs of F-ISB values different with Fig 2c. Therefore, it is not reliable to simply select one of the four pairs of F-ISB values as the estimated F-ISB. However, this problem can be solved reliably by using the multi-dimensional particle filter approach described in section 3.

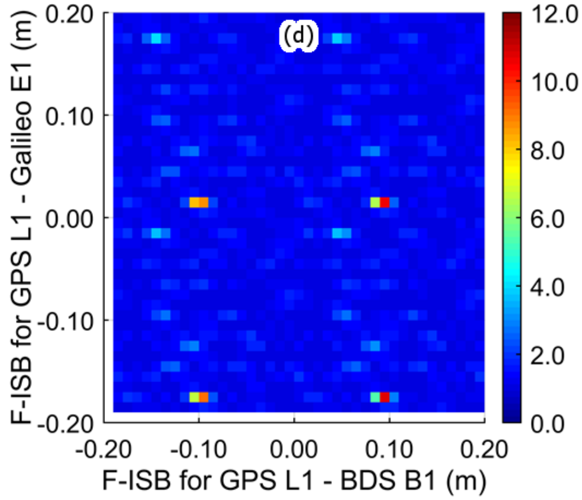

Fig. 3 RATIO distribution in the integration of GEB_L1 for baseline TLSG-TLSE at epoch 3:39:00 on DOY 001 of 2015 employing only 3 GPS, 2 Galileo and 3 BDS satellites (c)

5 The results from multi-dimensional particle filter approach

The multi-dimensional particle filter approach proposed in section 3 is validated in this section with the three integration cases e.g. GEJ_L5, GE_L1L5 and GEB_L1 as examples. Firstly, all the observed satellites are used to estimate the correct F-ISB values. The RATIO values are calculated based on GNSS single-epoch data processing. Secondly, this approach is carried out in real data but simulated scenarios, where only a few satellites from each GNSS system are observed, to test the performance of the proposed multi-dimensional particle filter approach under challenging observation conditions.

F-ISB estimation with all the observed satellites

In this section, the F-ISB parameters are estimated with all the observed satellites. We employ 200 particles in the two-dimensional particle filter approach because we have tested that this number is adequate to get the F-ISBs estimated quickly and reliably. The STD of the state noise in Eq.(15) is set to 0.003 m in this experiment.

We first test the F-ISB estimation in the integration of GEJ_L5 where the F-ISB for GPS L5 and Galileo E5a as well as one F-ISB for GPS L5 and QZSS L5 is needed. The data for SIN0-SIN1 on DOY 007 of 2016 with epoch interval of 30 s are employed. Because only very few

GPS satellites have L5 observations, the GPS L1 observations are also used in this estimation to derive a reliable single-epoch solution.

The process converges within four epochs and the particles at each epoch are shown in the Fig. 4. It shows that the 200 particles gradually concentrate to the area with larger RATIO values and eventually the estimated F-ISBs converge to the true F-ISB values. During the filtering process, the particles can freely move around and are not limited within [-0.2, 0.2] m. The half-cycle problem appears in the multi-dimensional case in Fig. 4(c) and is well solved by the cluster analysis method implemented on each dimension of the particles, as shown in Fig. 4(d). Figure 5 shows the estimation which converges at the 4^{th} epoch with a STD < 8 mm. The estimated F-ISB for DOY 007 of 2016 are shown in the Fig. 6(a).

The estimation of F-ISB for GE_L1L5 integration is also conducted by using the data from baseline TLSG-TLSE collected on DOY 007 of 2016. The estimated results are presented in Fig. 6(b). For the third example, the estimated F-ISBs for GEB_L1 integration for about 6 hours, where at least one satellite from each system is observed, are shown in Fig. 6(c). The frequencies of GPS L1 and BDS B1 are slightly different. In the ambiguity fixing strategy described in section 2, the corresponding approximate ISB value estimated with code pseudorange observations is -0.3007 m.

The mean values of the estimated F-ISBs for GEJ_L5, GE_L1L5 and GEB_L1 with all observed satellites are presented in Table 1, along with the STD of the estimated F-ISB values for the whole data sets. The STD of F-ISB are calculated according to the estimated F-ISB value series.

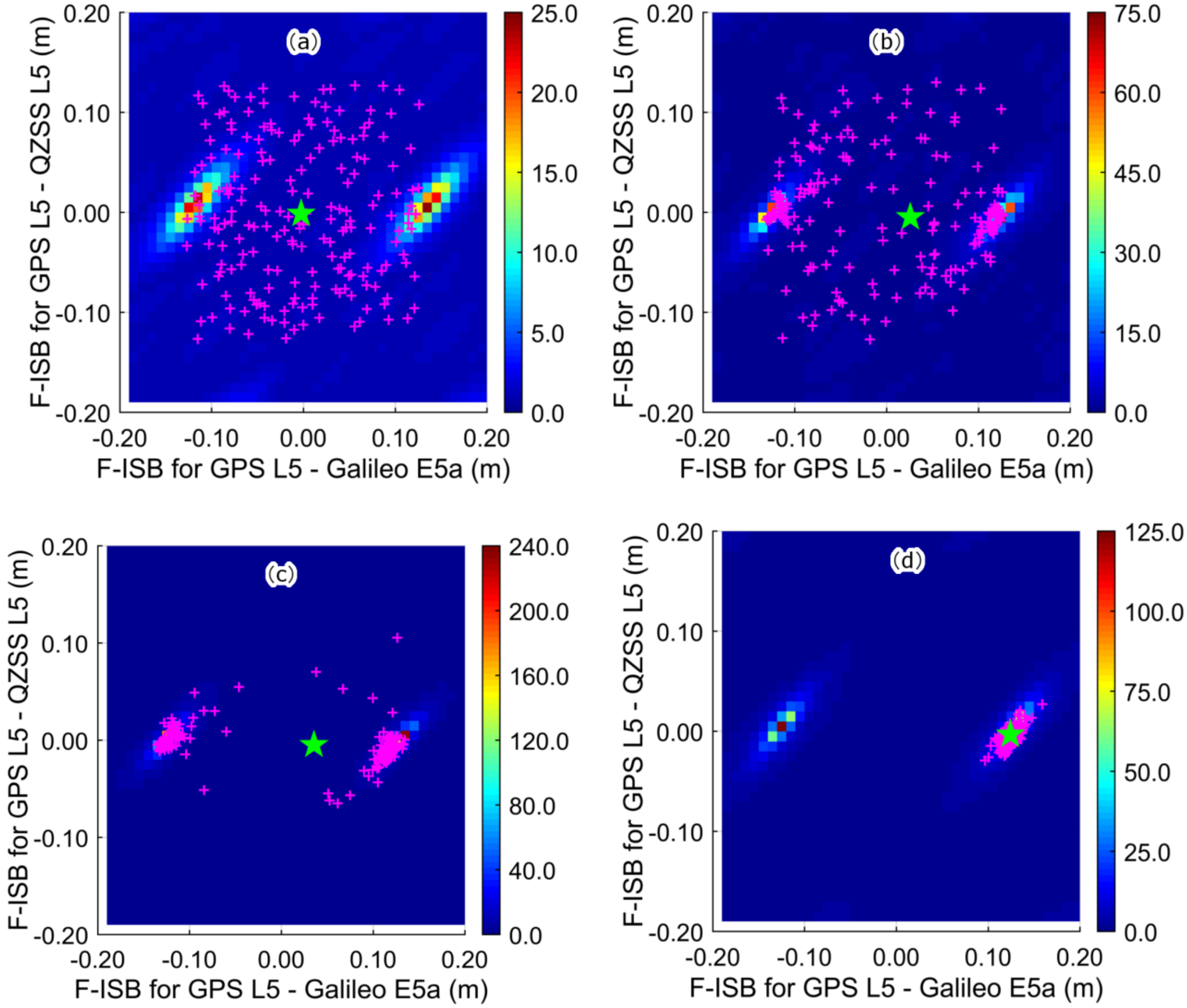

Fig. 4 Convergence process of the two-dimensional particle filter approach for GEJ_L5 integration on the zero-baseline SIN0-SIN1. The pink crosses indicate the particles and the green star refers to the estimated value according to the particles.

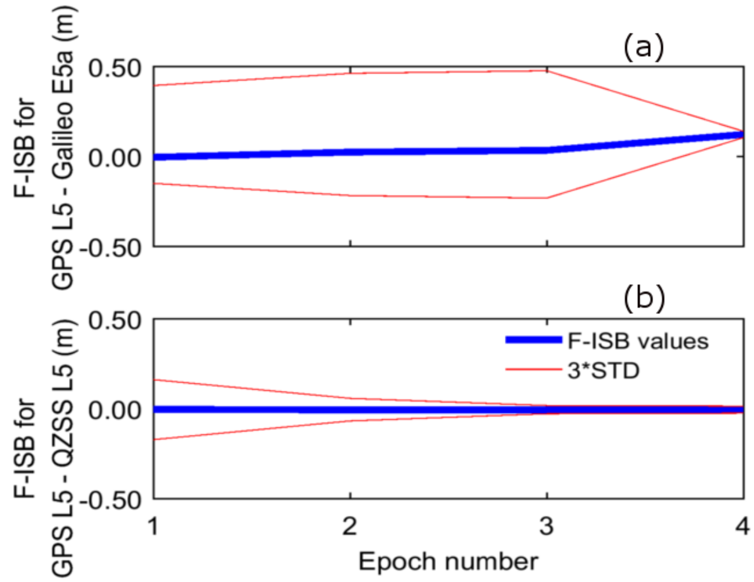

Fig. 5 Estimated F-ISB results for GPS L1 and BDS B1 (*a*), GPS L1 and Galileo E1 (*b*) corresponding to the process presented in Fig. 3.

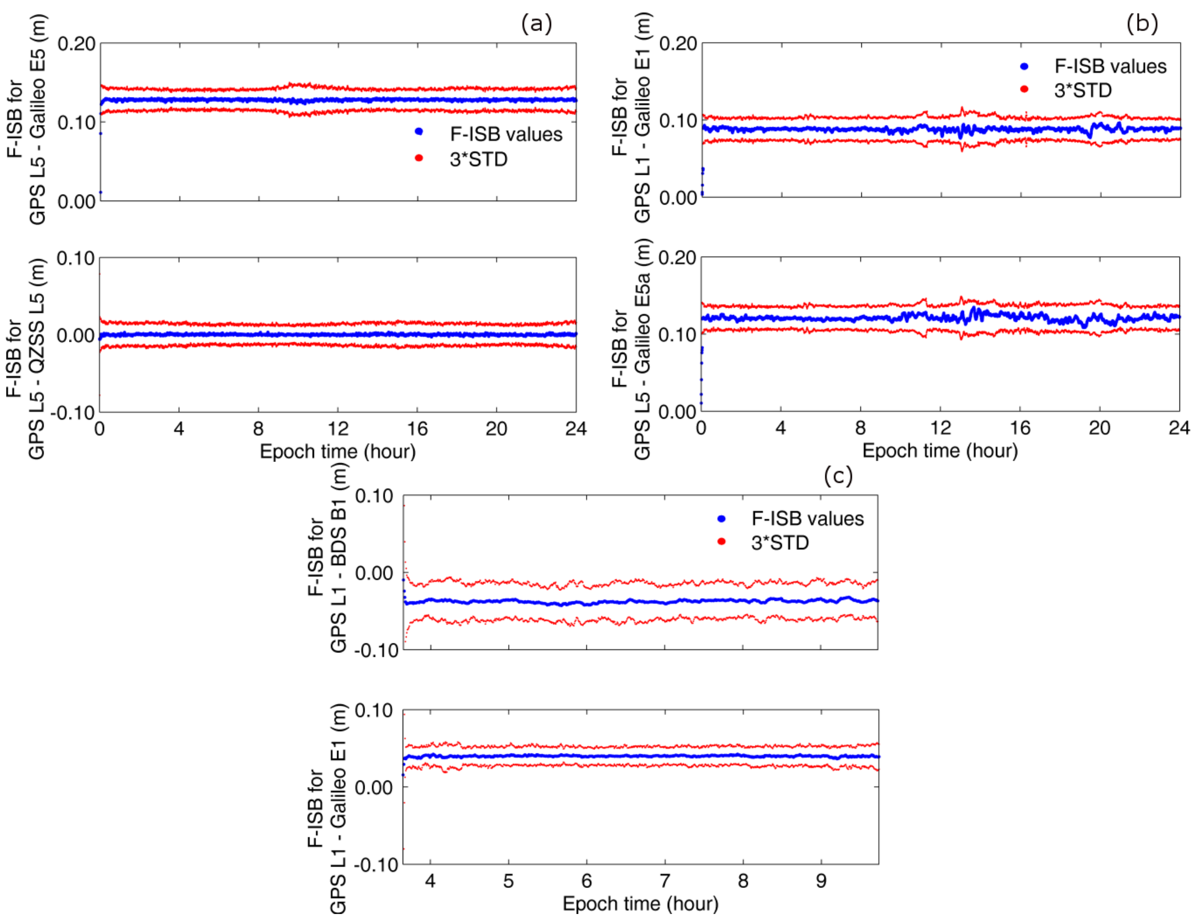

Fig. 6 Estimated F-ISBs for integration of GEJ_L5 for baseline SIN0-SIN1 (a), integration of GE_L1L5 for baseline TLSG-TLSE (b), and integration of GEB_L1 for baseline TLSG-TLSE (c)

Table 1 Mean values and STDs of the estimated F-ISB series

System Integration	F-ISB of each combination	With all satellites		With less satellites	
		Mean F-ISB (m)	STD of F-F-ISB (m)	Mean F-ISB (m)	STD of F-F-ISB (m)
GEJ_L5	GPS L5 – Galileo E5a	0.1281	0.0009	-0.1286	0.0017
	GPS L5 – QZSS L5	0.0002	0.0008	0.0005	0.0101
GE_L1L5	GPS L1 – Galileo E1	0.0880	0.0024	0.0871	0.0036
	GPS L5 – Galileo E5a	0.1207	0.0034	0.1199	0.0042
GEB_L1	GPS L1– Galileo E1	0.0398	0.0008	0.0389	0.0016
	GPS L1 – BDS B1	-0.0377	0.0019	-0.0394	0.0016

F-ISB Estimation with Fewer Observed Satellites by Simulating Challenging Observation Scenarios

To investigate the performance of the two-dimensional approach under challenging observation conditions, observation scenarios with a small number of observed satellites from each system are simulated. Because it is difficult for even the particle approach to determine the true value of each F-ISB under such challenging conditions, the number of particles is increased to 500 in the experiment.

For GEJ_L5 integration, a scenario with a total of six satellites (one QZSS satellite, all the GPS satellites with L5 signals, and the rest satellites from Galileo) is tested. The satellite pseudo random noise (PRN) number is depicted in Fig.7(a). The data from 5:29:00 to 5:51:30, from 9:27:30 to 10:54:30, from 22:34:30 to 24:00:00 are missing because during that period less than six satellites with L5 signal are observed. Two phase F-ISB parameters are estimated simultaneously using the two-dimensional particle filter approach described in Section 3, while the two pseudorange ISB are parameterized and estimated in real time in the data processing.

The estimated results are presented in Fig.7(b), where it takes around 30 minutes to converge. It can also be observed that the STDs of the weighted particles vary with time. This is probably due to the variation of satellite conditions, such as change of elevation angles with time. The F-ISB plot in Fig.7(b) is below zero unlike the plot in Fig. 6(a) due to the period character.

Adding the L5 wavelength 0.2548 m to the values in Fig. 7(b) can change the estimated F-ISBs to positive values.

After the two carrier phase F-ISB values are determined, the baseline solutions can be derived. Since the estimated F-ISB are fixed as known values, both intra- and inter-system DD-ambiguities can be fixed together. Thus, this strategy is referred to as *intra and inter DDAF* (DD-Ambiguity Fixing). For comparison, the same observations are also processed where only intra-system DD-ambiguities are fixed (without inter-system models), named *intra only DDAF*. For the *intra only DDAF* strategy, there are only three integer DD-ambiguities, instead of five for the *intra and inter DDAF* strategy. The positioning errors for both intra only DDAF and intra and inter DDAF strategies are shown in Fig.7(c), which shows that the intra and inter DDAF strategy can produce much better positioning results.

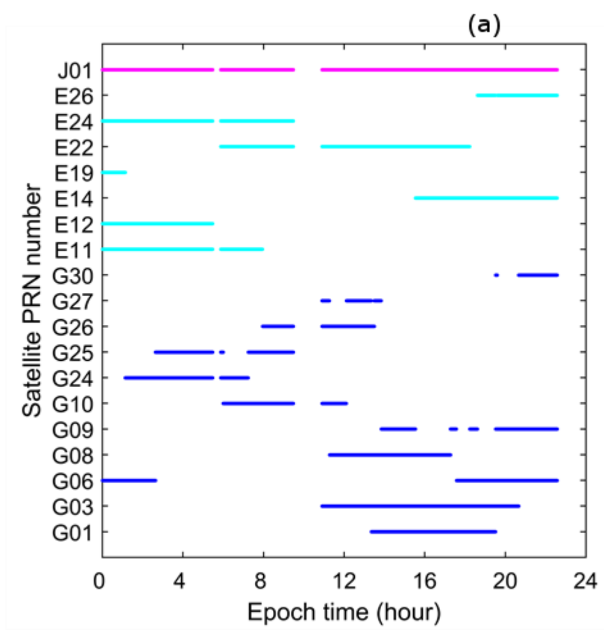

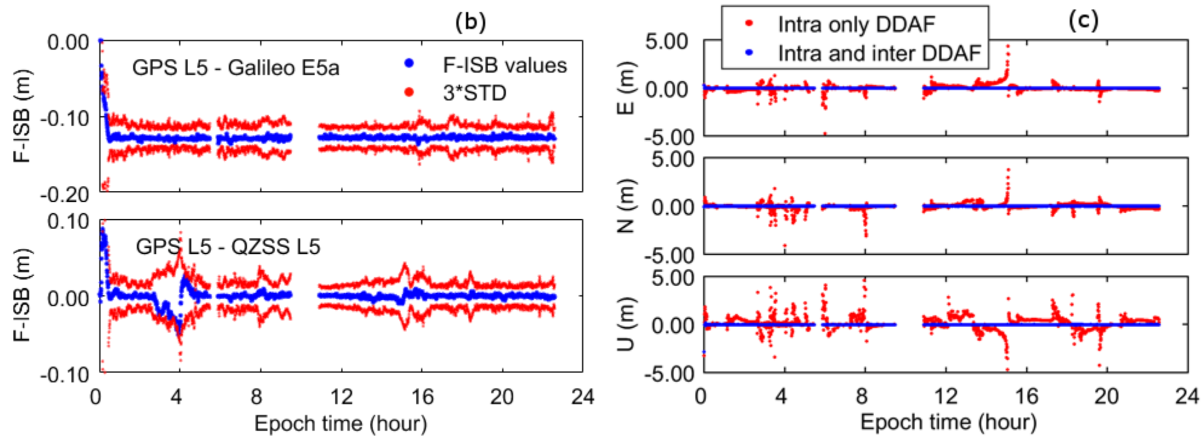

Fig. 7 The PRN of the satellites (a), estimated F-ISB and the particle STD (b) and the biases in positioning results (c) for GEJ_L5 integration of baseline SIN0-SIN1

In the ambiguity resolution procedure, the RATIO test threshold is set as 3. At some epochs, the fixing RATIO is larger than the threshold, but the errors of the baseline fixed solution are still larger than 3 cm. In this case, the ambiguity resolution cannot be considered to be successful. Thus, we add a solution check criterion to examine whether or not the positioning errors are larger than 3 cm. Fig.7(c) shows that the ambiguity fixing success rate is 99.7% for intra and inter DDAF strategy, and it is only 19.3% for intra only DDAF strategy. The success rates with and without solution check for the *intra and inter DDAF* strategy and *intra only DDAF* strategy are listed in Table 2.

In the experiment with GE_L1L5 and GEB_L1 integrations, the baseline TLSG-TLSE is a non-zero baseline. The pseudorange ISB can be easily estimated using a few epochs of data. The pseudorange ISB are then set as known parameters and only the carrier phase F-ISB parameters are estimated in the next step data processing.

For the GE_L1L5 integration, a scenario of five satellites, including 2 to 4 GPS satellites and the rest being Galileo satellites, is tested. The PRNs of satellites are presented in Fig.8(a). The estimated F-ISB are presented in Fig.8(b). The positioning errors for *intra only DDAF* and *intra and inter DDAF* strategies are shown in Fig.8(c). The ambiguity fixing success rates for the two DDAF strategies are presented in Table 2.

The F-ISB estimation for GEB_L1 integration is also tested, with two satellites selected from each system i.e. six satellites in total from GPS, Galileo and BDS systems. As the Galileo and BDS constellations are still in development, approximately only six hours of data on DOY 001 of 2015 can meet the satellite selection requirement. The satellite PRNs, estimated F-ISB, and the positioning errors are presented in Fig.9(a), Fig.9 (b) and Fig.9 (c), respectively. The ambiguity fixing success rates for the two strategies are presented in the last row of Table 2.

The mean values of the estimated F-ISBs of all the three combinations with less satellites are given in Table 1. The STDs of the F-ISB series are also listed. Although the STD of the F-ISB series with less satellites are relatively larger due to fewer observations, the mean F-ISB values are close to the values estimated with all observed satellites.

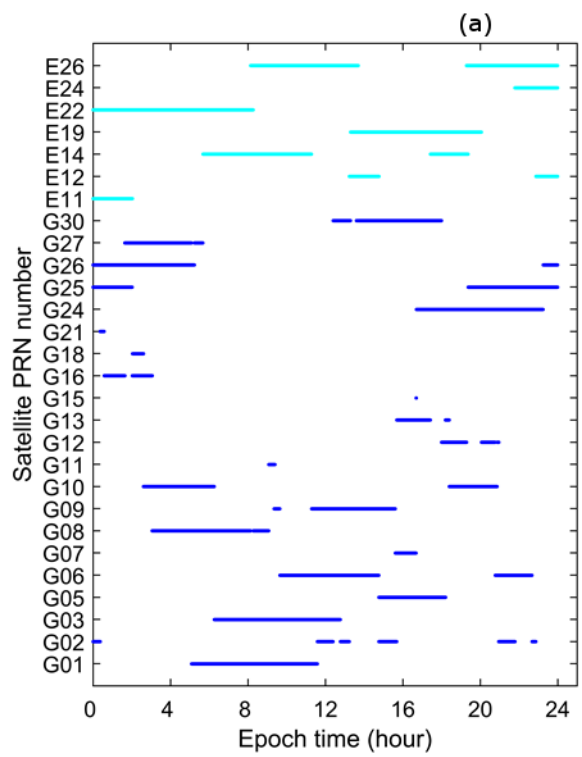

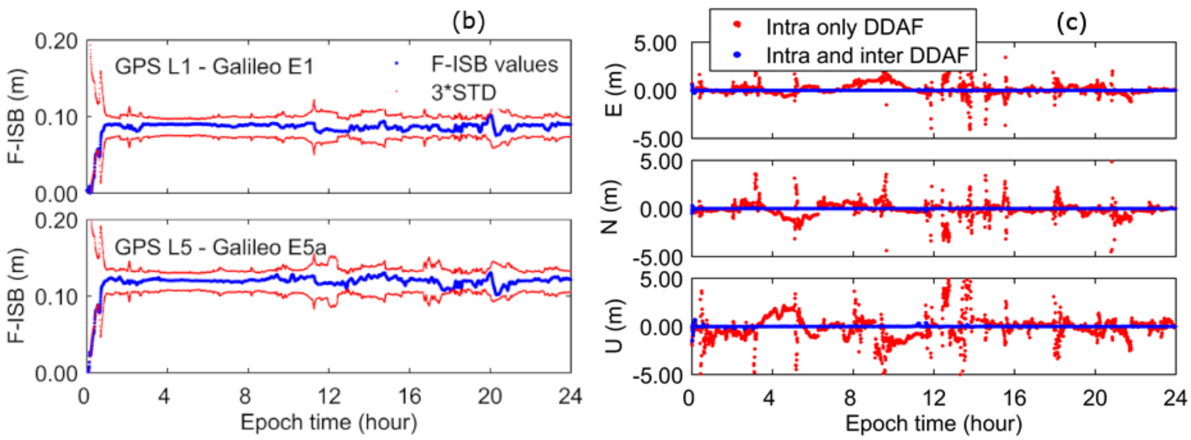

Fig. 8 The PRNs of the satellites (a), estimated F-ISB and the particle STD (b) and the positioning errors (c) for GE_L1L5 integration of baseline TLSG-TLSE

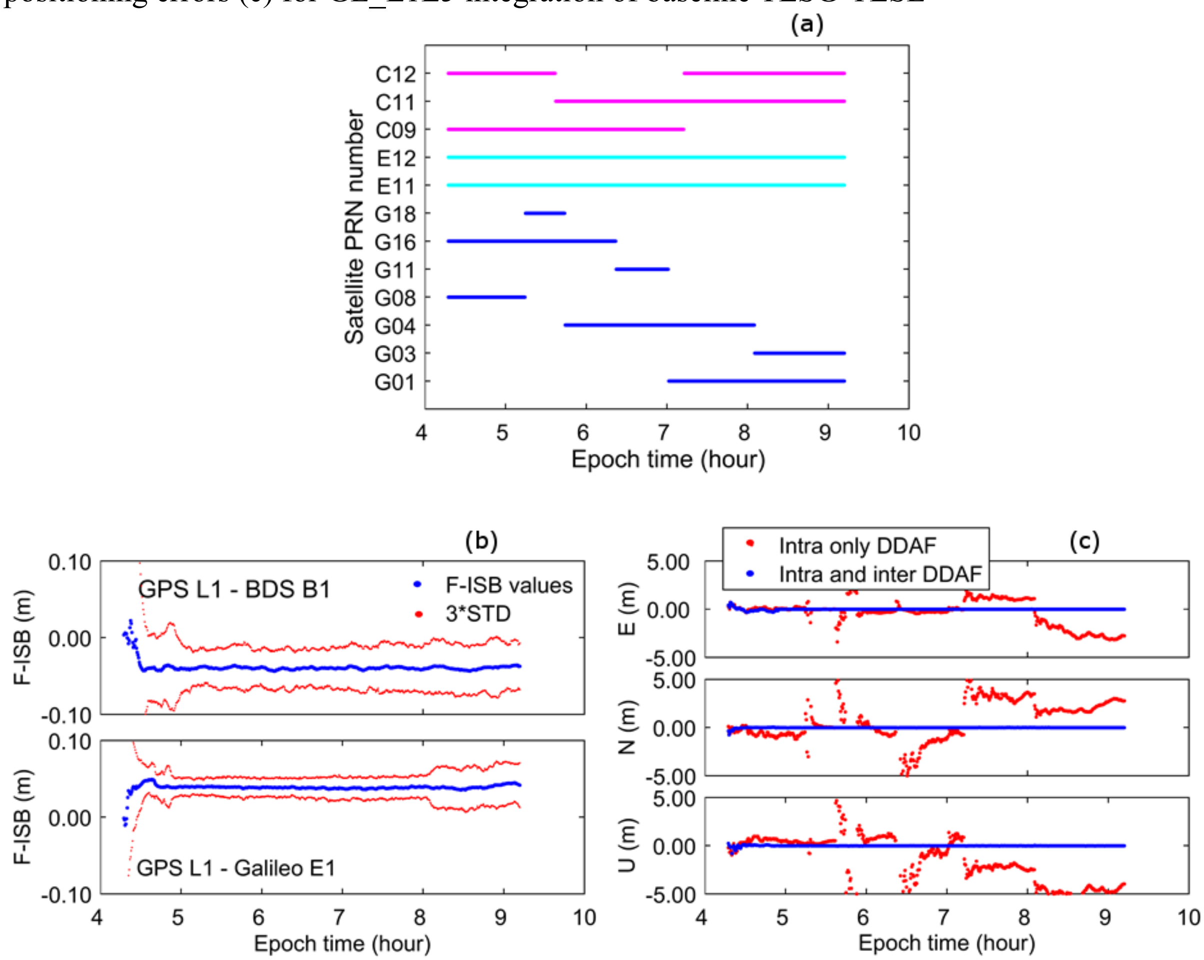

Fig. 9 PRN of the satellites (a), estimated F-ISB and the particle STD (b) and the biases in positioning results (c) for GEB_L1 integration of baseline TLSG-TLSE

Table 2 Empirical success rates for the integration of the three combinations

			With solution check		Without solution check	
Frequency combination	Baseline	Number of satellites	Intra and inter DDAF	Intra only DDAF	Intra and inter DDAF	Intra only DDAF
GEJ_L5	SIN0-SIN1	6	99.7%	19.3%	99.7%	41.0%
GE_L1L5	TLSG-TLSE	5	95.6%	3.4%	95.6%	5.9%
GEB_L1	TLSG-TLSE	6	88.1%	0.0%	88.5%	7.8%

6 Discussion

In traditional methods, the F-ISB are estimated along with ambiguities. Due to the rank-deficiency caused by the F-ISB and ambiguity parameters the integer inter-system ambiguities cannot help in the estimation (Odijk and Teunissen 2013a). In the traditional F-ISB estimation methods, only after the intra-system ambiguity−fixed solutions are derived, can accurate F-ISB values be estimated. However intra-system ambiguity−fixed solutions have a low success rate when the number of satellites is small. For example, the success rate of the fixed solutions is only 19.3% for GEJ_L5 integration in the above experiment. If we relax the requirement and allow the positioning error to be larger than 3 cm, the success rate can increase to 41.0% for GEJ_L5 integration as shown in Table 2. The other integration examples show similar results. Because the baseline true distances are usually unknown in practice, increasing the success rate of ambiguity-fixed baseline solutions by relaxing the requirement of < 3 cm in the intra only DDAF strategy is not reliable.

Even if the RATIO value is large, the estimated F-ISB might still not be correct. On the contrary, using the proposed multi-dimensional particle filter approach, the ambiguity fixing success rate of baseline solution is remarkably increased with the *intra and inter DDAF* strategy. For example, it is 99.7% for the GEJ_L5 integration. Moreover, the ambiguity fixing success rate of baseline solution is the same regardless of the implementation of the requirement of positioning error < 3 cm. Therefore, the proposed multi-dimensional particle filter approach has a much higher reliability for F-ISB estimation.

7 Conclusions

In challenging observation scenarios where the number of observed satellites is small, the fixing of inter-system DD-ambiguities is difficult. However, this problem can be alleviated with the assistance of known ISB parameters. Therefore, estimation of ISB parameters, especially the carrier phase F-ISB, is very helpful in such a situation. The particle filter approach generates F-ISB samples in advance for F-ISB estimation. With the F-ISB samples that are close to the true values, the inter-system DD-ambiguities can be fixed to integers.

This paper proposed a multiple-dimensional particle filter approach for F-ISB estimation, which is an improvement over the existing one-dimensional one. This allows the estimation of two or more F-ISB at the same time. In the F-ISB estimation, more inter-system DD integer ambiguities, which are independent of intra-system DD-ambiguities, can be fixed to integers simultaneously. This will significantly enhance the GNSS positioning and navigation accuracy and reliability. The merit of this multi-dimensional approach is more obvious when the number of observed satellites from each constellation is small.

The multi-dimensional particle filter approach is tested with three experiments, including GPS L5, Galileo E5a and QZSS L5 integration, GPS and Galileo L1, E1 and L5, E5a integration, GPS L1, Galileo E1 and BDS B1 integration. The result shows that two independent F-ISB parameters in each integration combination can be accurately estimated simultaneously. More importantly, when the number of observed satellites from each constellation is small, the strategy of intra and inter DDAF has dramatically higher success rate than the strategy of intra only DDAF. For example, in the GPS L5, Galileo E5a and QZSS L5 integration with a total of six satellites from three systems, the success rate is improved from 19.3% in intra only DDAF strategy to 99.7% in intra and inter DDAF strategy. In the intra only DDAF strategy, although the ambiguity fixing passes the RATIO test, the corresponding GNSS positioning solution still likely have a large error (> 3 cm). It shows that the estimated F-ISB parameters may not be so precise or reliable with the traditional F-ISB estimation methods. However, with the proposed multi-dimensional particle filter approach, the two F-ISB values can be determined more reliably.

This proposed method has demonstrated a superior performance. When more GNSS constellation systems are available, the more advantages this multi-dimensional particle filter approach will have. With the emergence of more new satellite signals and more global and regional GNSS systems, this approach will play a more important role in the high precision carrier phase-based GNSS positioning with multi-GNSS system integration.

Acknowledgments

Zhizhao Liu thanks the support of Hong Kong Research Grants Council (RGC) project (PolyU 5203/13E, B-Q37X) and Hong Kong Polytechnic University (projects 152103/14E, 152168/15E, and 1-BBYH) and the grant supports from the Key Program of the National Natural Science Foundation of China (project No.: 41730109). Yumiao Tian is supported by the Young Scientists Fund of the National Natural Science Foundation of China (project No.: 41804022) and the Fundamental Research Funds for the Central Universities (2682018CX33).

References

Blewitt G (1989) Carrier phase ambiguity resolution for the global positioning system applied to geodetic baselines up to 2000 km. J Geophys Res, 94(B8):10187-10203

Candy J (2009) Bayesian signal processing: Classical, modern and particle filtering methods. John Wiley & Sons, Inc., Hoboken, New Jersey, US

Dach, R., Brockmann, E., Schaer, S., Beutler, G., Meindl, M., Prange, L., et al. (2009). GNSS processing at CODE: status report. Journal of Geodesy , 83(3-4), 353-365

Dong D, Bock, Y (1989) Global positioning system network analysis with phase ambiguity resolution applied to crustal deformation studies in California. J Geophys Res, 94(B4):3949-3966

Doucet A, Freitas, N, Gordon, N (2001) Sequential Monte Carlo Methods in Practice. Springer, New York

Euler H, Schaffrin B (1991) On a measure of discernibility between different ambiguity solutions in the static-kinematic GPS-mode. Proceedings of the international symposium on kinematic systems in Geodesy, surveying, and remote sensing. Springer, Berlin Heidelberg New York, pp. 285-295

Force, D., & Miller, J. (2013). Combined Global Navigation Satellite Systems in the Space Service Volume. Proceedings of the ION International Technical Meeting.

Ge M, Gendt G, Rothacher M, Shi C, Liu J (2008) Resolution of GPS carrier-phase ambiguities in precise point positioning (PPP) with daily observations. Journal of Geodesy, 82(7):389-399

Gordon J, Salmond J, Smith F (1993) Novel approach to nonlinear/non-Gaussian Bayesian state estimation. IEE Proceedings on Radar and Signal Processing, 140(2):107-113

Gustafsson F, Gunnarsson F, Bergman N, Forssell U, Jansson J, Karlsson R, Nordlund P (2002) Particle filters for Positioning, Navigation, and Tracking. IEEE transactions on Signal Processing, 50(2):425-437

Haug A (2012) Bayesian Estimation and Tracking: A Practical Guide. Wiley & Sons Press, New Jersey

Ineichen , D., Brockmann , E., & Schaer, S. (2008). Processing combined GPS/GLONASS data at swisstopo's local analysis center. Proceedings of EUREF Symposium.

Julien, O., Alves, P., Cannon, E. M., & Zhang, W. (2003). A tightly coupled GPS/GALILEO combination for improved ambiguity resolution. Proceedings of the European Navigation Conference , (S. 1-14).

Khodabandeh A, Teunissen P (2016) PPP-RTK and inter-system biases: the ISB look-up table as a means to support multi-system PPP-RTK, J Geod (2016) 90:837–851. DOI: 10.1007/s00190-016-0914-9

Kozlov D, Tkachenko M (1997) Instant RTK cm with Low Cost GPS+ GLONASS [TM] C/A Receivers. Proceedings of ION GPS 1997, Kansas City, MO, September 1997, pp. 1559-1570

Kubo N, Tokura H, Pullen S (2018) Mixed GPS-BeiDou RTK with inter-systems bias estimation aided by CSAC, GPS Solutions, 22:5. DOI: 10.1007/s10291-017-0670-1

Leick A (1998) GLONASS satellite surveying. Journal of Surveying Engineering, 124(2):91-99

Li, X., Ge, M., Dai, X., Ren, X., Mathias , F., & Jens, W. (2015). Accuracy and reliability of multi-GNSS real-time precise positioning: GPS, GLONASS, BeiDou, and Galileo. Journal of Geodesy, 607-635.

Melgard T, Tegedor J, Jong K, Lapucha D, Lachapelle G (2013) Interchangeable integration of GPS and Galileo by using a common system clock in PPP. Proceedings of ION GNSS, Nashville, TN, September 2013, pp. 16-20

Odijk, D., & Teunissen, P. J. (2013a). Characterization of between-receiver GPS-Galileo inter-system biases and their effect on mixed ambiguity resolution. GPS solutions, 17(4), 521-53.

Odijk, D., & Teunissen, P. J. (2013b). Estimation of differential inter-system biases between the overlapping frequencies of GPS, Galileo, BeiDou and QZSS. Proceedings of the 4th International Colloquium Scientific and Fundamental Aspects of the Galileo Programme, (S. 4-6). Prague, Czech Republic.

Odolinski, R., Teunissen, P. J., & Odijk, D. (2014). Combined BDS, Galileo, QZSS and GPS single-frequency RTK. GPS solution, 19(1),151-163.

Paziewski , J., Sieradzki , R., & Wielgosz , P. (2015). Selected properties of GPS and Galileo-IOV receiver intersystem biases in multi-GNSS data processing. Measurement Science and Technology, 26(9) 095008.

Paziewski, J., & Wielgosz, P. (2015). Accounting for Galileo-GPS inter-system biases in precise satellite positioning. Journal of Geodesy, 89(1),81-93.

Teunissen P (1996) GPS carrier phase ambiguity fixing concepts. In Kleusberg A, Teunissen P, GPS for geodesy, pp. 263-336, Springer, Berlin Heidelberg New York

Tian, Y., Ge, M., & Neitzel, F. (2015). Particle filter-based estimation of inter-frequency phase bias for real-time GLONASS integer ambiguity resolution. Journal of Geodesy, 89(11):1145-1158.

Tian, Y., Ge, M., & Neitzel, F. (2016). Particle filter-based estimation of inter-system phase bias for multi-GNSS integer ambiguity resolution. GPS Solutions, DOI 10.1007/s10291-016-0584-3.

Tian Y, Liu Zhizhao, Ge M, Neitzel F (2017). Determining inter-system bias of GNSS signals with narrowly spaced frequencies for GNSS positioning. Journal of Geodesy, DOI: 0.1007/s00190-017-1100-4

Verhagen S, Teunissen P (2013) The ratio test for future GNSS ambiguity resolution. GPS Solutions, 17(4):535-548

Wang J, Rizos C, Stewart M, Leick A (2001) GPS and GLONASS integration: modeling and ambiguity resolution issues. GPS Solutions, 5(1):55-64